

Solid State and Solution Studies of Lanthanide(III) Complexes of Cyclohexanetriols, Models of the Coordination Sites Found in Sugars

Pascale Delange,^{*,†} Christian Husson,[†] Colette Lebrun,[†] Jacques Pécaut,[‡] and Philippe J. A. Vottéro[†]

Laboratoire Reconnaissance Ionique et Matériaux Moléculaires and Laboratoire Métalloprotéines, Magnétisme et Modèles Chimiques, Service de Chimie Inorganique et Biologique, Département de Recherche Fondamentale sur la Matière Condensée, CEA-Grenoble, 17, avenue des Martyrs, 38 054 Grenoble cedex 9, France

Received October 19, 2000

This report covers studies in trivalent lanthanide complexation by two simple cyclohexanetriols that are models of the two coordination sites found in sugars and derivatives. Several complexes of trivalent lanthanide ions with *cis,cis*-1,3,5-trihydroxycyclohexane (**L**₁) and *cis,cis*-1,2,3-trihydroxycyclohexane (**L**₂) have been characterized in the solid state, and some of them have been studied in organic solutions. With **L**₁, Ln(**L**₁)₂ complexes are obtained when crystallization is performed from acetonitrile solutions whatever the nature of the salt (nitrate or triflate) [Ln(**L**₁)₂(NO₃)₂](NO₃) (Ln = Pr, Nd); [Ln(**L**₁)₂(NO₃H₂O)](NO₃)₂ (Ln = Eu, Ho, Yb); [Ln(**L**₁)₂(OTf)₂(H₂O)](OTf) (Ln = Nd, Eu). Lanthanum nitrate itself gives a mixed complex [La(**L**₁)₂(NO₃)₂][La**L**₁(NO₃)₄] from acetonitrile solution while [La(**L**₁)₂(NO₃)₂](NO₃) is obtained using dimethoxyethane as reaction solvent and crystallization medium. With **L**₂, Ln(**L**₂)₂ complexes have also been crystallized from methanol solution [Ln(**L**₂)₂(NO₃)₂](NO₃) (Ln = Pr, Nd, Eu). Single-crystal X-ray diffraction analyses are reported for these complexes. Complex formation in solution has been studied for several triflate salts (La, Pr, Nd, Eu, and Yb) with **L**₁ and **L**₂, respectively in acetonitrile and in methanol. In contrast to the solid state, both structures Ln(**L**) and Ln(**L**)₂ equilibrate in solution, as was demonstrated by low-temperature ¹H NMR and electrospray ionization mass spectrometry experiments. Competing experiments in complexing abilities of **L**₁ and **L**₂ with trivalent lanthanide cations have shown that only **L**₂ exhibits a small selectivity (Nd > Pr > Yb > La > Eu) in methanol.

Introduction

Lanthanide(III) species exhibit rich and unique spectroscopic and magnetic properties, and rare-earth compounds are used for numerous applications, as relaxation agents in nuclear magnetic resonance imaging,^{1,2} as luminescent probes in biology and medicine^{3,4} or as catalysts for the cleavage of RNA and DNA.^{5,6} In another field, the separation of trivalent lanthanides from actinides in acidic aqueous solutions issued from nuclear fuel reprocessing by liquid liquid extraction is still a challenge despite progress made in the past decade.⁷ This is especially true if one wants to avoid the presence of such elements as sulfur or phosphorus in the coordinating molecules. Ionic radii and the relevant chemical properties of rare earths and actinides such as americium and curium in the trivalent oxidation state

are very similar.⁸ Both series have a good affinity for oxygen ligands. We decided to investigate the coordination chemistry of lanthanide cations with some model ligands in the solid state and in solution to have better insight into the parameters controlling the complexation in the phases of extraction. Polyols are examples of simple model oxygen-donor ligands.

The coordination of metal cations by polyols in aqueous solution has been extensively studied in the carbohydrate and cyclitol fields over the past four decades. Several reports have reviewed the subject.^{9–12} S. J. Angyal demonstrated that only two specific sites were able to give metal complexes in water: 1,3,5-triaxial and 1,2,3-axial, equatorial, axial trihydroxy sites.^{13,14} The two simple molecules *cis,cis*-1,3,5- and *cis,cis*-1,2,3-trihydroxycyclohexanes, respectively named **L**₁ and **L**₂ throughout this work, are convenient models to compare the affinity of lanthanide hard ions to the different coordination sites identified by S. J. Angyal in inositols.

We reported, in a previous publication,¹⁵ the complexation of europium(III) salts by **L**₁ and **L**₂. Both ligands, each

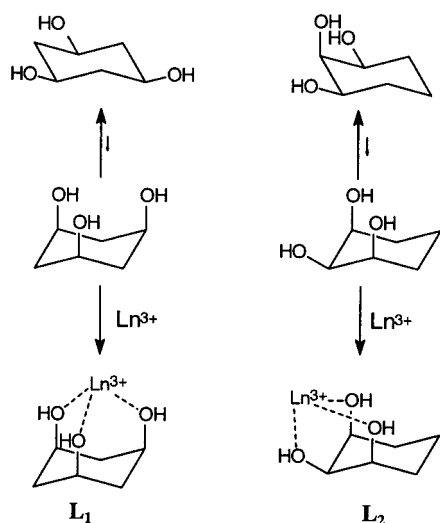
[†] Laboratoire Reconnaissance Ionique et Matériaux Moléculaires.

[‡] Laboratoire Métalloprotéines, Magnétisme et Modèles Chimiques.

- (1) Aime, S.; Botta, M.; Fasano, M.; Terreno, E. *Chem. Soc. Rev.* **1998**, 27, 19–29.
- (2) Comblin, V.; Gilsoul, D.; Hermann, M.; Humblet, V.; Jacques, V.; Mesbahi, M.; Sauvage, C.; Desreux, J.-F. *Coord. Chem. Rev.* **1999**, 185–186, 451–470.
- (3) Bünzli, J.-C. G. In *Lanthanide Probes in Life, Chemical and Earth Sciences*; Bünzli, J.-C. G., Choppin, G. R., Eds.; Elsevier: Amsterdam, 1989; pp 219–293.
- (4) Elhabiri, M.; Scopelliti, R.; Bünzli, J.-C. G.; Piguet, C. *J. Am. Chem. Soc.* **1999**, 121, 10747–10762.
- (5) Bruce, T. C.; Tsubouchi, A.; Dempcy, R. O.; Olson, L. P. *J. Am. Chem. Soc.* **1996**, 118, 9867–9875.
- (6) Oh, S. J.; Choi, Y.-S.; Hwangbo, S.; Bae, S. C.; Ku, J. K.; Park, J. W. *Chem. Commun.* **1998**, 2189–2190.
- (7) Nash, K. L. In *Separations of f Elements*; Nash, K. L., Ed.; Plenum Press: San Diego, CA, 1994; pp 1–8.

- (8) Rizkalla, E. N.; Choppin, G. R. In *Handbook on the Physics and Chemistry of Rare-Earths*; Gschneidner, K. A., Jr., Eyring, L., Choppin, G. R., Lander, G. H., Eds.; Elsevier Science: Amsterdam, 1994; Vol. 18, pp 529–558.
- (9) Rendleman, J. A. *Adv. Carbohydr. Chem.* **1966**, 21, 209–271.
- (10) Angyal, S. J. *Adv. Carbohydr. Chem.* **1992**, 47, 1–43.
- (11) Hegetschweiler, K. *Bol. Soc. Chil. Quim.* **1997**, 42, 257–279.
- (12) Gyurcsik, B.; Nagy, L. *Coord. Chem. Rev.* **2000**, 203, 81–149.
- (13) Angyal, S. J. *Tetrahedron* **1974**, 30, 1695–1702.
- (14) Angyal, S. J.; Greeves, D.; Pickles, V. A. *Carbohydr. Res.* **1974**, 35, 135–173.

Scheme 1



possessing three hard donor hydroxyl groups, are able to complex the europium(III) cation in organic solvents. As already noted *cis,cis*-1,3,5- and *cis,cis*-1,2,3-trihydroxycyclohexanes **L**₁ and **L**₂ may be considered as configurationally but not spatially preorganized, according to the respective thermodynamic stabilities of their chair conformation. A chair inversion is thus necessary to organize the three binding sites prior to complexation (Scheme 1). Lanthanide complexes with **L**₂ are formed in methanol, whereas those with **L**₁ exist in acetonitrile but are unstable in protic solvents. This behavior has been explained by the greater reorganization energy involved in the case of complexation by **L**₁ in comparison to **L**₂.¹⁶ In the case of lanthanide(III) complexation by **L**₁ in methanol, the stabilization due to the metal complex formation is probably too weak to counterbalance the energetic cost of conformational reorganization which is necessary to move three hydroxyl groups from equatorial to axial position.

This contribution deals with lanthanide(III) complexes of the two simple oxygen-donor ligands **L**₁ and **L**₂ along the 4f series. We report both structural studies in the solid state and in solution. Various rare-earth complexes were crystallized and characterized by X-ray diffraction. Species in solution have been qualitatively determined by electrospray ionization mass spectrometry for La and Eu, and a quantitative analysis has been done by low-temperature ¹H NMR for four paramagnetic lanthanide cations (Pr, Nd, Eu, and Yb). ¹H NMR competition experiments between two different cations give an estimation of the selectivity of these two ligands along the 4f series.

Experimental Section

Syntheses and Characterization of Complexes. Hydrated lanthanide salts, *cis,cis*-1,3,5-trihydroxycyclohexane (**L**₁) and *cis,cis*-1,2,3-trihydroxycyclohexane (**L**₂), were purchased respectively from Aldrich and TCI and were used without further purification. Analyses for C, H, and N were carried out by the Service Central de Microanalyses (CNRS). Five different methods of crystallization have been used to prepare complexes depending on the nature of the salts and on the stability of the complexes in protic solvents.

Method A. To a solution of Ln(OTf)₃ (0.25 mmol) in acetonitrile (5 mL) was added **L**₁·2H₂O (0.084 g, 0.5 mmol). After stirring until

dissolution of the ligand was complete (10 min), the complex was isolated by crystallization induced by slow diffusion of diethyl ether.

Method B. To a solution of Ln(NO₃)₃·6H₂O (0.25 mmol) in acetonitrile (10 mL) was added **L**₁·2H₂O (0.084 g, 0.5 mmol). After stirring under reflux during 5 min the medium was filtered on occasion. The complex crystallized on cooling.

Method C. To a solution of **L**₂ (0.132 g, 1.0 mmol) in methanol (4 mL) was added a solution of Ln(NO₃)₃·6H₂O (0.5 mmol) in methanol (1 mL). Slow diffusion of diethyl ether induced crystallization of the complex from the solution.

Method D. To a solution of Ln(NO₃)₃·6H₂O (0.25 mmol) in dimethoxyethane (10 mL) was added **L**₁·2H₂O (0.084 g, 0.5 mmol). After 20 min of stirring under reflux the medium was decanted or filtered. The solid residue was dissolved at reflux in dimethoxyethane and left for crystallization after addition of a small quantity of acetonitrile (less than 5%). The complex crystallized also on cooling from the supernatant.

[Pr(L₁)₂(NO₃)₂](NO₃)·(CH₃CN), **1 (B):** Pr(NO₃)₃·5H₂O (0.210 g, 0.5 mmol); **L**₁·2H₂O (0.169 g, 1.0 mmol). Pale green crystals. Yield: 58%.

[Nd(L₁)₂(NO₃)₂](NO₃), **2 (B):** Nd(NO₃)₃·5H₂O (0.211 g, 0.5 mmol); **L**₁·2H₂O (0.169 g, 1.0 mmol). Pale pink crystals. Yield: 56%.

[Eu(L₁)₂(NO₃)(H₂O)](NO₃)₂, **3 (B):** Eu(NO₃)₃·5H₂O (0.215 g, 0.5 mmol); **L**₁·2H₂O (0.169 g, 1.0 mmol). Colorless crystals. Yield: 68%.

[Ho(L₁)₂(NO₃)(H₂O)](NO₃)₂, **4 (B):** Ho(NO₃)₃·5H₂O (0.220 g, 0.5 mmol); **L**₁, 2H₂O (0.169 g, 1.0 mmol). White crystals. Yield: 74%.

[Yb(L₁)₂(NO₃)(H₂O)](NO₃)₂, **5 (B):** Yb(NO₃)₃·5H₂O (0.225 g, 0.5 mmol); **L**₁·2H₂O (0.169 g, 1.0 mmol). Colorless crystals. Yield: 79%.

[Nd(L₁)₂(OTf)₂(H₂O)](OTf), **6 (A):** Nd(OTf)₃·H₂O (0.301 g, 0.5 mmol); **L**₁·2H₂O (0.169 g, 1.0 mmol). Pink crystals. Yield: 72%.

[Eu(L₁)₂(OTf)₂(H₂O)](OTf), **7 (A):** Eu(OTf)₃·H₂O (0.305 g, 0.5 mmol); **L**₁·2H₂O (0.169 g, 1.0 mmol). Colorless crystals. Yield: 72%.

[Pr(L₂)₂(NO₃)₂](NO₃), **8 (C):** **L**₂ (0.132 g, 1.0 mmol); Pr(NO₃)₃·5H₂O (0.210 g, 0.5 mmol). Pale green crystals. Yield: 66%.

[Nd(L₂)₂(NO₃)₂](NO₃), **9 (C):** **L**₂ (0.132 g, 1.0 mmol); Nd(NO₃)₃·5H₂O (0.211 g, 0.5 mmol). Pink crystals. Yield: 75%.

[Eu(L₂)₂(NO₃)₂](NO₃), **10 (C):** **L**₂ (0.132 g, 1.0 mmol); Eu(NO₃)₃·5H₂O (0.215 g, 0.5 mmol). Colorless crystals. Yield: 48%.

[La(L₁)₂(NO₃)₂][La(L₁)₂(NO₃)₄](H₂O), **11 (B):** **L**₁ (0.84 g, 0.5 mmol); La(NO₃)₃·5H₂O (0.81 g, 0.25 mmol). Colorless crystals. Yield: 46%.

[La(L₁)₂(NO₃)₂](NO₃)·(0.5CH₃CN), **12 (D):** **L**₁ (0.84 g, 0.5 mmol); La(NO₃)₃·5H₂O (0.81 g, 0.25 mmol). Colorless crystals. Yield: 67%.

X-ray Crystallographic Analyses of Complexes 1–12. All the crystals were analyzed using a Bruker SMART CCD area detector three-circle diffractometer (Mo K α radiation, graphite monochromator, $\lambda = 0.71073 \text{ \AA}$). The cell parameters were obtained with intensities detected on three batches of 15 frames with exposure time between 5 and 30 s. The crystal–detector distance was 6 cm. For three settings of Φ and 2Θ , 1268 narrow data frames were collected for 0.3° increments in ω with exposure time between 5 and 30 s. A full hemisphere of data was collected for each complex. At the end of data collection, the first 50 frames were recollected to establish that crystal decay had not taken place during the collection. Unique intensities with $I > 10\sigma(I)$ detected on all frames using the SAINT program¹⁷ were used to refine the values of the cell parameters. Lorentz and polarization corrections were made. The substantial redundancy in data allowed empirical absorption corrections to be applied using multiple measurements of equivalent reflections with the SADABS Bruker program.¹⁸ Space groups were determined from systematic absences, and they were confirmed by the successful solution of the structure (Table 1). Complete information on crystal data and data collection parameters are given in the Supporting Information.

The structures were solved by the direct methods program SHELXL-TL,¹⁹ which revealed most of the complex atoms. Difference Fourier synthesis led to the location of all remaining non-hydrogen atoms. All non-hydrogen atoms were anisotropically refined on F^2 , and hydrogen

(15) Husson, C.; Delangle, P.; Pécaut, J.; Vottéro, P. J. A. *Inorg. Chem.* **1999**, *38*, 2012–2019.

(16) Eliel, E. L.; Wilen, S. H. *Stereochemistry of Organic Compounds*; John Wiley and Sons: New York, 1994; pp 706–708.

(17) *SMART and SAINT Area-Detector and Integration Software*; Siemens Analytical X-Ray Instruments Inc.: Madison, WI, 1995.

(18) *SADABS, Bruker Area Detector Absorption Corrections Software*; Bruker Analytical X-Ray Systems: Wissembourg, France, 1998.

Table 1. Selected Crystallographic Data

	1	2	4	5	6	8	9	11	12
formula	$[\text{Pr}(\text{L}_1)_2(\text{NO}_3)_2](\text{NO}_3)(\text{CH}_3\text{CN})$	$[\text{Nd}(\text{L}_1)_2(\text{NO}_3)_2](\text{NO}_3)(\text{CH}_3\text{CN})$	$[\text{Ho}(\text{L}_1)_2(\text{NO}_3)_2](\text{H}_2\text{O})(\text{NO}_3)_2$	$[\text{Yb}(\text{L}_1)_2(\text{NO}_3)_2](\text{H}_2\text{O})(\text{NO}_3)_2$	$[\text{Nd}(\text{L}_1)_2(\text{OTf})_2](\text{H}_2\text{O})(\text{OTf})$	$[\text{Pr}(\text{L}_2)_2(\text{NO}_3)_2](\text{NO}_3)$	$[\text{Nd}(\text{L}_2)_2(\text{NO}_3)_2](\text{NO}_3)$	$[\text{La}(\text{L}_1)_2(\text{NO}_3)_2](\text{H}_2\text{O})$ $[\text{La}(\text{L}_1)(\text{NO}_3)_4](\text{H}_2\text{O})$	$[\text{La}(\text{L}_1)_2(\text{NO}_3)_2](\text{NO}_3)$ $[\text{La}(\text{L}_1)_2(\text{NO}_3)_2](\text{NO}_3)_2$
fw	632.31	635.64	633.29	641.40	873.78	591.25	594.58	1064.36	609.78
cryst syst	monoclinic	monoclinic	monoclinic	monoclinic	monoclinic	monoclinic	monoclinic	monoclinic	monoclinic
space group	$P2_1$	$P2_1$	Cc	Cc	$P2_1/n$	$P2_1/c$	$P2_1/c$	$P2_1$	$P2_1/n$
<i>a</i> , Å	9.8833(5)	9.8771(2)	16.787(5)	16.857(5)	10.73580(10)	14.4589(2)	14.4172(4)	9.3430(4)	12.2964(16)
<i>b</i> , Å	9.6719(5)	9.6617(3)	8.155(2)	8.150(2)	19.0206(2)	12.13790(10)	12.0804(3)	19.9349(5)	10.3191(15)
<i>c</i> , Å	12.1136(7)	12.0966(3)	15.632(6)	15.732(6)	15.05040(10)	13.30840(10)	13.2703(3)	10.3519(4)	17.533(4)
β , deg	107.2900(10)	107.3130(10)	107.69(4)	107.92(4)	105.2990(10)	116.1350(10)	116.1280(10)	109.9880(10)	98.085(10)
<i>V</i> , Å ³	1105.62(10)	1102.07(5)	2038.7(11)	2056.7(12)	2964.40(5)	2096.83(4)	2075.05(9)	1811.92(11)	2202.6(6)
<i>Z</i>	2	2	4	4	4	4	4	2	4
<i>D</i> _{calc} , g/cm ³	1.899	1.915	2.063	2.071	1.958	1.873	1.903	1.951	1.839
μ (Mo K α), mm ⁻¹	2.287	2.440	3.970	4.635	2.087	2.403	2.583	2.435	2.020
temp, K	193(2)	293(2)	293(2)	293(2)	293(2)	293(2)	293(2)	193(2)	298(2)
data/param	3632/416	3164/403	2233/289	2953/290	5020/502	3754/386	3759/377	4965/487	5313/415
R1/wR2 ^a	0.0231/0.0578	0.0235/0.0584	0.0450/0.1064	0.0324/0.0816	0.0395/0.1049	0.0223/0.0565	0.0323/0.0819	0.0400/0.0985	0.0258/0.0681

^a Structure was refined on F_o^2 using all data: $wR2 = [\sum w(F_o^2 - F_c^2)^2]^{1/2}$, where $w^{-1} = [\sigma(F_o^2) + (aP)^2 + bP]$ and $P = [\max(F_o, 0) + 2F_c]^{1/2}$.

atoms were isotropically refined for complexes **1–3**, **6–10**, and **12** and geometrically fixed for compounds **4**, **5**, and **11**. Final *R* indices and residual electronic density are listed in Table 1.

ES-MS. The mass spectrometry was performed on a Quattro II triple-quadrupole spectrometer (Micromass), equipped with an electrospray source. The source temperature was set at 80 °C. The electrospray probe (capillary) voltage was optimized in the range of 3.5–5 kV for positive ion electrospray. The sample cone voltage was set within the range 40–90 V. Complexes in solution were infused in MeOH or in MeCN (depending on the ligand), through a fused silica tubing, using a syringe pump at a flow rate in the range 5–10 $\mu\text{L min}^{-1}$. In the electrospray mass spectrometric (ES-MS) data given below, only the *m/z* peaks corresponding to the most abundant isotopic mass have been indicated. For tandem mass spectrometry experiments (MS/MS), argon was used as the collision gas.

NMR Experiments. Lanthanide nitrates and triflates were dried under vacuum for several days, and their lanthanide content was then determined by chelatometric titration with EDTA and xylenol orange as the indicator. Deuterated methanol (Merck, 99.8 atom % D) and acetonitrile (Merck, 99 atom % D) were used as received. The samples for NMR spectroscopy were prepared by dissolving the ligands and the lanthanide salt in 700 μL of deuterated solvent. The NMR spectra were recorded using AM 400 Bruker or Unity 400 Varian spectrometers. Spectra were calibrated by assigning the residual solvent signal a shift from TMS of 3.38 ppm (methanol) and 2.00 ppm (acetonitrile). Longitudinal relaxation rates were measured using a nonselective inversion recovery pulse sequence;²⁰ T_1 values were obtained from a three-parameter fit of the data to an exponential recovery function. 2D COSY spectra were recorded in magnitude mode²¹ with recycle delays optimized for fast-relaxing species.²² 2D NOESY experiments were recorded in phase sensitive mode.²³ The mixing times were 50 ms for complexes with **L**₁ and 10 ms for complexes with **L**₂.

Results and Discussion

Crystal Structures of Complexes 1–12. All complexes (**1–10**) crystallize with 1:2 metal to ligand stoichiometry whatever the nature of the metal, the salt, or the ligand. Therefore the six hydroxyl groups of ligands contribute to the first coordination sphere. Lanthanum offers an intriguing case. Crystallizing the complex according to method **B**, only a mixed complex incorporating $\text{La}(\text{L}_1)_2$ and $\text{La}(\text{L}_1)$ entities is isolated (**11**). On changing the solvent for DME (1,2-dimethoxyethane) and applying method (**D**) we were able to isolate crystals of $\text{La}(\text{L}_1)_2$ only (**12**). The structures of complexes **1–12** were determined by X-ray crystallography, and the europium complexes **3**, **7**, and **10** have been discussed in a previous publication.¹⁵

Complexes **1–10** may be assigned to four different structural types. In all these complexes, the metal coordination number is nine and the coordination polyhedron is a tricapped trigonal prism. Complexes $[\text{Pr}(\text{L}_1)_2(\text{NO}_3)_2](\text{NO}_3)$ (**1**) and $[\text{Nd}(\text{L}_1)_2(\text{NO}_3)_2](\text{NO}_3)$ (**2**) are isostructural, and accordingly only the neodymium complex is shown in Figure 1. The lanthanide coordination sphere contains the six hydroxyl groups of the two ligand **L**₁ molecules, one bidentate nitrate, and one monodentate nitrate. Figure 2 shows the complex $[\text{Yb}(\text{L}_1)_2(\text{NO}_3)(\text{H}_2\text{O})](\text{NO}_3)_2$ (**5**) which is isostructural to $[\text{Eu}(\text{L}_1)_2(\text{NO}_3)(\text{H}_2\text{O})](\text{NO}_3)_2$ (**3**) and $[\text{Ho}(\text{L}_1)_2(\text{NO}_3)(\text{H}_2\text{O})](\text{NO}_3)_2$ (**4**) and very similar to

(19) Sheldrick, G. M. *SHELXTL-Plus, Version 5.1. Structure Determination Software Programs*; Siemens Analytical X-ray Instruments Inc.: Madison, WI, 1998.

(20) Vold, R. L.; Waugh, J. S.; Klein, M. P.; Phelps, D. E. *J. Chem. Phys.* **1968**, *48*, 3831–3832.

(21) Ave, W. P.; Bartholdi, E.; Ernst, R. R. *J. Chem. Phys.* **1976**, *64*, 2229–2235.

(22) Keating, K. A.; de Ropp, J. S.; La mar, G. N.; Balch, A. L.; Shiau, F.-Y.; Smith, K. M. *Inorg. Chem.* **1991**, *30*, 3258–3263.

(23) Macura, S.; Ernst, R. R. *Mol. Phys.* **1980**, *41*, 95–117.

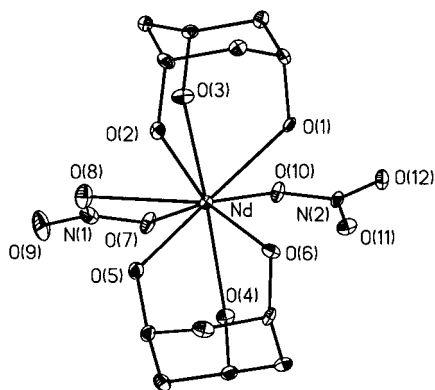


Figure 1. ORTEP drawing of **2** with labelling schemes. Thermal ellipsoids for non-hydrogen atoms are drawn at the 30% probability level.

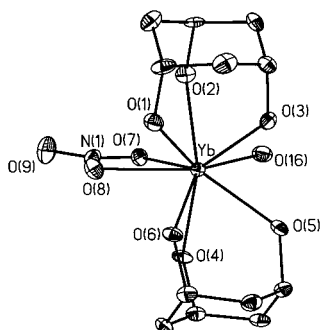


Figure 2. ORTEP drawing of **5** with labelling schemes. Thermal ellipsoids for non-hydrogen atoms are drawn at the 30% probability level.

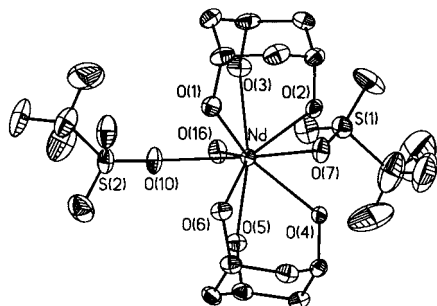


Figure 3. ORTEP drawing of **6** with labelling schemes. Thermal ellipsoids for non-hydrogen atoms are drawn at the 30% probability level.

complexes **1** and **2** with the monodentate nitrate replaced by a water molecule. $[\text{Nd}(\text{L}_1)_2(\text{OTf})_2(\text{H}_2\text{O})](\text{OTf})$ (**6**) and $[\text{Eu}(\text{L}_1)_2(\text{OTf})_2(\text{H}_2\text{O})](\text{OTf})$ (**7**) are examples of lanthanide triflate complexes in which the lanthanide ion is coordinated by the six hydroxyl groups of the two ligand L_1 molecules, two monodentate triflates, and one water molecule. The neodymium complex is presented in Figure 3. Figure 4 shows the complex $[\text{Pr}(\text{L}_2)_2(\text{NO}_3)_2](\text{NO}_3)$ (**8**) which is isostructural to $[\text{Nd}(\text{L}_2)_2(\text{NO}_3)_2](\text{NO}_3)$ (**9**) and $[\text{Eu}(\text{L}_2)_2(\text{NO}_3)_2](\text{NO}_3)$ (**10**). Two ligands L_2 are coordinating the lanthanide ion, with a bidentate and a monodentate nitrate. Selected interatomic distances are given in Table 2 for complexes **1**–**10**. Comparison of the mean distance of the metal to oxygen atoms of the ligands L_1 in complexes **1**–**5** shows that there is a steady decreasing of this distance when the atomic number increases (Pr^{3+} 2.492 Å; Nd^{3+} 2.477 Å; Eu^{3+} 2.433 Å; Ho^{3+} 2.388 Å; Yb^{3+} 2.375 Å) corresponding to the decreasing of the ionic radius of the ion. The same trend is observed with the distances of Ln^{3+} –O for

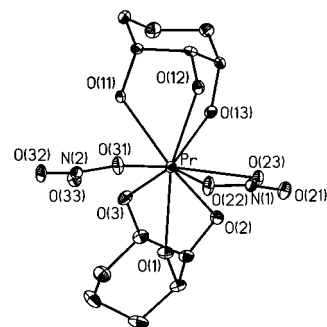


Figure 4. ORTEP drawing of **8** with labelling schemes. Thermal ellipsoids for non-hydrogen atoms are drawn at the 30% probability level.

the bidentate nitrate. In complexes **3**–**5** the decrease in the value of the Ln – OH_2 bond lengths from Eu (**3**) to Yb (**5**) is 0.09 Å. This value is in agreement with the expected contraction of 0.08 Å calculated from Shannon ionic radii for 9-coordinated ions.²⁴ The substitution of a monodentate nitrate (1 and 2) for a water molecule (**3**–**5**) in the first coordination sphere probably originates from steric constraints arising with the so-called lanthanoids contraction. The two monodentate triflates in the first coordination sphere of complexes **6** and **7** are probably responsible for the dissymmetry observed in the Ln^{3+} –O distances in the coordination of the two ligands. The three complexes **8**–**10** belong to the same structural type and here too, as in the case of L_1 , there is a regular decreasing of Ln^{3+} –O distances from Pr^{3+} to Eu^{3+} . The structural characteristics of **10** have been discussed in detail previously,¹⁵ and the same remarks may be made for **8** and **9**. The Ln^{3+} –O distances are also significantly longer for the equatorial hydroxyl groups (Pr^{3+} 2.587 Å; Nd^{3+} 2.565 Å; Eu^{3+} 2.534 Å) versus the axial ones (Pr^{3+} 2.467 Å; Nd^{3+} 2.447 Å; Eu^{3+} 2.407 Å).

Lanthanum complexes $[\text{La}(\text{L}_1)_2(\text{NO}_3)_2][\text{La}(\text{L}_1)(\text{NO}_3)_4]$ (**11**) and $[\text{La}(\text{L}_1)_2(\text{NO}_3)_2](\text{NO}_3)$ (**12**) deserve a particular treatment; their ORTEP drawings are respectively shown in Figures 5 and 6. Complex **11** is perhaps the most surprising one because two lanthanum complexes with different coordination spheres and numbers coexist in the crystal. The two lanthanum ions have thus a substantially different environment. On one hand $\text{La}(1)$ coordinates the three hydroxyl groups of the ligand and four bidentate nitrates thus giving rise to a coordination number of eleven, which is not common.²⁵ On the other hand $\text{La}(2)$ is coordinated to the six hydroxyl groups of the two molecules of ligands and the coordination sphere is completed to a coordination number of ten by two bidentate nitrates. The coordination polyhedron of $\text{La}(2)$ appears as a distorted tetradecahedron whose plane O(5)–O(51)–O(62)–O(61) has a distortion of ± 0.2 Å, plane O(4)–O(52)–O(9)–O(8)–O(6) has a distortion of ± 0.3 Å, while the two mean planes makes a dihedral angle of 6.9° . The same distortion in the coordination tetradecahedron is found for La in complex **12**. The distortions are of the same order: ± 0.3 Å for the square face O(3)–O(1)–O(22)–O(12) and ± 0.2 Å for the pentagonal face O(3)–O(1)–O(22)–O(13)–O(12) with a dihedral angle of 7.4° between the mean planes. This tetradecahedron may also be considered as a *cis*-bicapped cube.²⁶ Another possibility for $\text{La}(2)$ in **11** is to consider a tetracapped distorted trigonal prism O(51) capping the O(5)–O(52)–O(61) triangular face, O(6), O(8), O(62) capping the

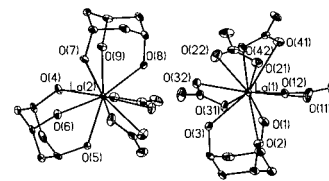
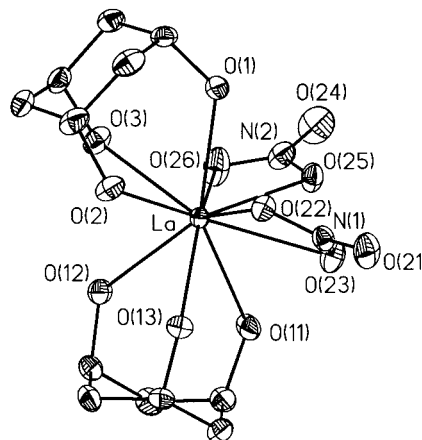
(24) Shannon, R. D. *Acta Crystallogr.* **1976**, A32, 751–767.

(25) Cotton, F. A.; Wilkinson, G. *Advanced Inorganic Chemistry*, 5th ed.; John Wiley and Sons: New York, 1988; pp 959–961.

(26) Favas, M. C.; Kepert, D. L. *Prog. Inorg. Chem.* **1981**, 28, 309–367.

Table 2. Selected Bond Lengths (Å) in Complexes 1–10 with Estimated Standard Deviations

1	2	3	4	5	6	7	8	9	10								
[Pr(L ₁) ₂ (NO ₃) ₂](NO ₃)·CH ₃ CN	[Nd(L ₁) ₂ (NO ₃) ₂](NO ₃)·CH ₃ CN	[Eu(L ₁) ₂ (NO ₃) ₂](NO ₃) ₂	[Ho(L ₁) ₂ (NO ₃) ₂](H ₂ O) ₂	[Yb(L ₁) ₂ (NO ₃) ₂](H ₂ O) ₂	[Nd(L ₁) ₂ (OTf) ₂](H ₂ O) ₂	[Eu(L ₁) ₂ (OTf) ₂](H ₂ O) ₂	[Pr(L ₂) ₂ (NO ₃) ₂](NO ₃)	[Nd(L ₂) ₂ (NO ₃) ₂](NO ₃)	[Eu(L ₂) ₂ (NO ₃) ₂](NO ₃)								
Pr–O(1)	2.470(3)	Nd–O(1)	2.4517(14)	Ho–O(1)	2.414(8)	Yb–O(1)	2.407(6)	Nd–O(1)	2.513(3)	Eu–O(1)	2.473(3)	Pr–O(1)	2.434(2)	Nd–O(1)	2.419(3)	Eu–O(1)	2.425(3)
Pr–O(2)	2.493(4)	Nd–O(2)	2.4012(12)	Ho–O(2)	2.351(8)	Yb–O(2)	2.335(6)	Nd–O(2)	2.456(2)	Eu–O(2)	2.414(2)	Pr–O(2)	2.5914(19)	Nd–O(2)	2.573(3)	Eu–O(2)	2.523(3)
Pr–O(3)	2.495(3)	Nd–O(3)	2.414(2)	Ho–O(3)	2.368(8)	Yb–O(3)	2.361(6)	Nd–O(3)	2.467(2)	Eu–O(3)	2.430(2)	Pr–O(3)	2.4661(19)	Nd–O(3)	2.447(3)	Eu–O(3)	2.427(3)
Pr–O(4)	2.482(3)	Nd–O(4)	2.416(2)	Ho–O(4)	2.384(10)	Yb–O(4)	2.390(7)	Nd–O(4)	2.526(2)	Eu–O(4)	2.495(2)	Pr–O(4)	2.477(2)	Nd–O(4)	2.453(3)	Eu–O(4)	2.372(3)
Pr–O(5)	2.486(3)	Nd–O(5)	2.4735(13)	Ho–O(5)	2.431(8)	Yb–O(5)	2.394(7)	Nd–O(5)	2.447(2)	Eu–O(5)	2.413(2)	Pr–O(5)	2.5830(19)	Nd–O(5)	2.557(3)	Eu–O(5)	2.544(3)
Pr–O(6)	2.524(4)	Nd–O(6)	2.508(3)	Ho–O(6)	2.380(9)	Yb–O(6)	2.362(6)	Nd–O(6)	2.470(2)	Eu–O(6)	2.424(2)	Pr–O(6)	2.4908(19)	Nd–O(6)	2.468(3)	Eu–O(6)	2.403(2)
Pr–O(7)	2.573(4)	Nd–O(7)	2.4869(13)	Ho–O(7)	2.450(9)	Yb–O(7)	2.448(6)	Nd–O(7)	2.471(2)	Eu–O(7)	2.431(2)	Pr–O(7)	2.6099(19)	Nd–O(7)	2.586(3)	Eu–O(7)	2.508(3)
Pr–O(10)	2.567(5)	Nd–O(8)	2.517(2)	Ho–O(8)	2.454(8)	Yb–O(8)	2.439(7)	Nd–O(8)	2.486(2)	Eu–O(8)	2.446(3)	Pr–O(10)	2.5648(19)	Nd–O(8)	2.542(3)	Eu–O(8)	2.560(3)
Pr–O(11)	2.578(3)	Nd–O(10)	2.566(2)	Ho–O(10)	2.377(8)	Yb–O(10)	2.331(7)	Nd–O(10)	2.478(2)	Eu–O(10)	2.438(2)	Pr–O(11)	2.580(2)	Nd–O(10)	2.556(3)	Eu–O(10)	2.519(3)

Figure 5. ORTEP drawing of **11** with labelling schemes. Thermal ellipsoids for non-hydrogen atoms are drawn at the 30% probability level.Figure 6. ORTEP drawing of **12** with labelling schemes. Thermal ellipsoids for non-hydrogen atoms are drawn at the 30% probability level.

three square faces. In this description the O(5)–O(52)–O(61) triangular face makes a dihedral angle of 14.5° with the mean plane formed by O(6), O(8), O(62) which in turn makes a dihedral angle of 1.7° with the second triangular face O(4)–O(7)–O(9). For La(1) in **11**, it is possible to find a capped tetradecahedron as coordination polyhedron. The pentagonal plane O(2)–O(31)–O(32)–O(42)–O(41)–O(11) is distorted by ±0.2 Å and the square plane O(1)–O(3)–O(22)–O(21) by ±0.02 Å, the two mean planes making a dihedral angle of 10.5°. Two other planes may also be considered, the pentagonal plane O(1)–O(2)–O(12)–O(41)–O(21), which is distorted by ±0.25 Å, and the square plane O(3)–O(31)–O(42)–O(22), distorted by ±0.16 Å, the two mean planes making a dihedral angle of 5.4°. The Ln³⁺–O distances with ligands **L**₁ are somewhat different around La(1) (2.534–2.577 Å) and La(2) (2.493–2.621 Å). They are comparable to the same distances in **12** (2.524–2.551 Å). Selected interatomic distances are shown in Table 3 for complexes **11** and **12**. It seems that the rise of La(2)–O distance distribution originates from steric constraints in the mixed complex **11**. The Ln³⁺–O bonds with the coordinated nitrates are of the same order around lanthanum in **12** (2.595–2.756 Å) and La(2) in **11** (2.604–2.732 Å) and also around La(1) but with a larger distribution (2.571–2.787 Å).

Many strong H-bonds are present in all these complexes as it is common for crystalline adducts between polyols and inorganic salts according to the large quantity of donor and acceptor groups.²⁷ They are found within the complex itself or between the complex and counteranions or solvent molecules. They reinforce its stability or the stability of the overall lattice. Only short hydrogen bonds with H–O distances between 1.74 and 2.39 Å are considered here, but several other hydrogen bonds are also present. As already seen in the case of the

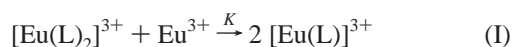
(27) Cook, W. J.; Bugg, C. E. *Metal-Ligand Interactions in Organic Chemistry and Biochemistry*; Reidel Publishing Company: Dordrecht, 1977; Vol. 2, pp 231–236.

Table 3. Selected Bond Lengths (Å) in Complexes **11** and **12** with Estimated Standard Deviations

11		12	
[La(L ₁) ₂ (NO ₃) ₂][La(L ₁)(NO ₃) ₄]		[La(L ₁) ₂ (NO ₃) ₂](NO ₃)·0.5CH ₃ CN	
La(1)–O(1)	2.542(6)	La–O(1)	2.5513(7)
La(1)–O(2)	2.534(5)	La–O(2)	2.5245(6)
La(1)–O(3)	2.577(6)	La–O(3)	2.5502(6)
La(1)–O(11)	2.730(6)	La–O(11)	2.5490(6)
La(1)–O(12)	2.571(5)	La–O(12)	2.5378(7)
La(1)–O(21)	2.612(6)	La–O(13)	2.5367(6)
La(1)–O(22)	2.583(6)	La–O(22)	2.6870(6)
La(1)–O(31)	2.705(6)	La–O(25)	2.5952(6)
La(1)–O(32)	2.660(6)	La–O(26)	2.6841(7)
La(1)–O(41)	2.787(6)	La–O(23)	2.7560(7)
La(1)–O(42)	2.745(6)		
La(2)–O(4)	2.493(5)		
La(2)–O(5)	2.580(5)		
La(2)–O(6)	2.621(6)		
La(2)–O(7)	2.507(6)		
La(2)–O(8)	2.509(5)		
La(2)–O(9)	2.580(5)		
La(2)–O(51)	2.732(6)		
La(2)–O(52)	2.604(6)		
La(2)–O(61)	2.729(6)		
La(2)–O(62)	2.691(6)		

previously published analysis of europium complexes,¹⁵ the energy of several bonds in these complexes is unusual. Compounds **1–5** have at least three to four short hydrogen bonds around 2 Å which never implicate an O donor site of one of the coordinated nitrates. The only exception is the very weak H-bond (2.472 Å) of O(8) in **3** accepting H(5)–C(5). For compound **6** the observed H-bonds are very similar to those described for **7**. The same is true for **8** and **9** in comparison to **10**. For these compounds much stronger H-bonds are present compared to complexes with ligand L₁. Finally all hydrogen atoms of ligand hydroxyl groups are engaged in hydrogen bonds in **11**, but a special mention must be devoted to the water molecule O(10) which is simultaneously bonded with the ligand hydroxyl group O(7) and the nitrate group O(63) on La(2), and the nitrate group O(41) on La(1). This water molecule seems thus to favor the coexistence of the two different species in the unit cell and to maintain the cohesion of the overall structure. In comparison to the other complexes described here, **12** does not exhibit very strong H-bonds, the shortest being H(30)–O(28) at 2.038 Å and H(10)–O(29) at 2.069 Å between one of the two ligands and the noncoordinated nitrate.

Solution Coordination Studies of Ln(III) by L₁ in Acetonitrile and L₂ in Methanol. (a) Eu(III) Complexation. We have demonstrated by ¹H NMR at low temperature that ligand L₁ forms a mixture of Eu(L₁) and Eu(L₁)₂ complexes in acetonitrile.¹⁵ For triflates as counterions, the study of ¹H NMR spectra as a function of the metal-to-ligand ratio $\rho = \text{Eu}/\text{L}_1$ has shown that, first, the only species present in solution was Eu(L₁)₂ for $\rho = 0.5$ and, second, the main equilibrium was equilibrium I for $\rho > 0.5$. The thermodynamic constant of this equilibrium calculated from integrated intensities on the ¹H NMR spectrum at 233 K is $K = 7 \pm 1$. Complexation of



europium triflate with L₂ was investigated in methanol; the constant K at 233 K is 3.0 ± 0.4 . Only when nitrates are used

Table 4. ES-MS Intensities of Eu(OTf)₃ and L₁ Solutions in Acetonitrile^a

species	<i>m/z</i>	$\rho = 0.33$	$\rho = 0.5$	$\rho = 1$	$\rho = 2$
[Eu(L ₁) ₂ (OTf) ₂] ⁺	715	60	38	33	23
[Eu(L ₁) ₂ (H) ₋₁ (OTf)] ⁺	565	100	100	100	47
[Eu(L ₁) ₂ (H) ₋₂] ⁺	415	20	17	9	5
[Eu(L ₁)(OTf) ₂] ⁺	583			48	100
[Eu(L ₁)(H) ₋₁ (OTf)] ⁺	433			38	75

^a Total Eu concentration = 2×10^{-3} mol L⁻¹; $\rho = [\text{Eu}]_0/[\text{L}_1]_0$.

Table 5. ES-MS Intensities of Eu(OTf)₃ and L₂ Solutions in Methanol^a

species	<i>m/z</i>	$\rho = 0.33$	$\rho = 0.5$	$\rho = 1$	$\rho = 2$
[Eu(L ₂) ₂ (OTf) ₂] ⁺	715	62	62	53	15
[Eu(L ₂) ₂ (H) ₋₁ (OTf)] ⁺	565	100	100	100	22
[Eu(L ₂) ₂ (H) ₋₂] ⁺	415	8	8	22	18
[Eu(L ₂)(OTf) ₂] ⁺	583			57	70
[Eu(L ₁)(H) ₋₁ (OTf)] ⁺	433			99	100

^a Total Eu concentration = 2×10^{-3} mol L⁻¹; $\rho = [\text{Eu}]_0/[\text{L}_2]_0$.

Table 6. ES-MS Intensities of Eu(NO₃)₃ and L₂ Solutions in Methanol^a

species	<i>m/z</i>	$\rho = 0.5$	$\rho = 1$	$\rho = 2$
[Eu(L ₂) ₂ (NO ₃) ₂] ⁺	541	10	11	7
[Eu(L ₂) ₂ (H) ₋₁ (NO ₃)] ⁺	478	98	59	16
[Eu(L ₂) ₂ (H) ₋₂] ⁺	415	100	79	24
[Eu(L ₂)(NO ₃) ₂] ⁺	409	4	12	15
[Eu(L ₂)(H) ₋₁ (NO ₃)] ⁺	346	60	100	100

^a Total Eu concentration = 2×10^{-3} mol L⁻¹; $\rho = [\text{Eu}]_0/[\text{L}_2]_0$.

as counterions, the Eu(L₂)₂ complex dissociates in Eu(L₂) and free ligand according to equilibrium II with $K' = (2.5 \pm 0.6) \times 10^{-3}$. For $\rho = \text{Eu}/\text{L}_2 > 0.5$, the equilibrium constant K could be measured: $K = 5.1 \pm 0.4$. The relative stability of Eu(L₂)₂ and Eu(L₂) complexes is then dependent on the counterion: $K = 3.0$ (triflates) and 5.1 (nitrates).¹⁵ In the following NMR studies, triflates were used as counterions, and the only detected equilibrium was equilibrium I, corresponding to the evaluated constant K .

We undertook a mass spectrometry study to confirm the nature of the complexes present in solution and identified by NMR spectroscopy. Electrospray ionization mass spectrometry (ES-MS) has been shown to be an appropriate technique to characterize qualitatively preformed ions in solution²⁸ and has moreover been used for the identification of supramolecular coordination complexes.^{29–34} Solutions of lanthanide(III) salts and ligand L₁ or L₂ with a total europium(III) concentration of 2×10^{-3} mol L⁻¹ have been prepared under the following stoichiometric conditions: EuL₃, EuL₂, EuL, and Eu₂L. For a sample cone voltage of 60 V, only ions bearing one positive charge are detected. Intensities of signals on ES-MS spectra are listed in Tables 4–6. First, no Eu(L)₃ complex is ever detected. Second, with triflates as counterions only cations

- (28) Smith, R. D.; Loo, J. A.; Edmonds, C. G.; Barinaga, C. J.; Udseth, H. R. *Anal. Chem.* **1990**, *62*, 882–899.
 (29) Hopfgartner, G.; Piguët, C.; Henion, J. D.; Williams, A. F. *Helv. Chim. Acta* **1993**, *76*, 1759–1766.
 (30) Hopfgartner, G.; Vilbois, F.; Piguët, C. *Rapid Commun. Mass Spectrom.* **1999**, *13*, 302–306.
 (31) Hopfgartner, G.; Piguët, C.; Henion, J. D. *J. Am. Soc. Mass Spectrom.* **1994**, *5*, 748–756.
 (32) van den Bergen, A.; Colton, R.; Percy, M.; West, B. O. *Inorg. Chem.* **1993**, *32*, 3408–3411.
 (33) Katta, V.; Chowdhury, S. K.; Chait, B. T. *J. Am. Chem. Soc.* **1990**, *112*, 5348–5349.
 (34) Leize, E.; Van Dorsselaer, A.; Krämer, R.; Lehn, J.-M. *J. Chem. Soc., Chem. Commun.* **1993**, 990–993.

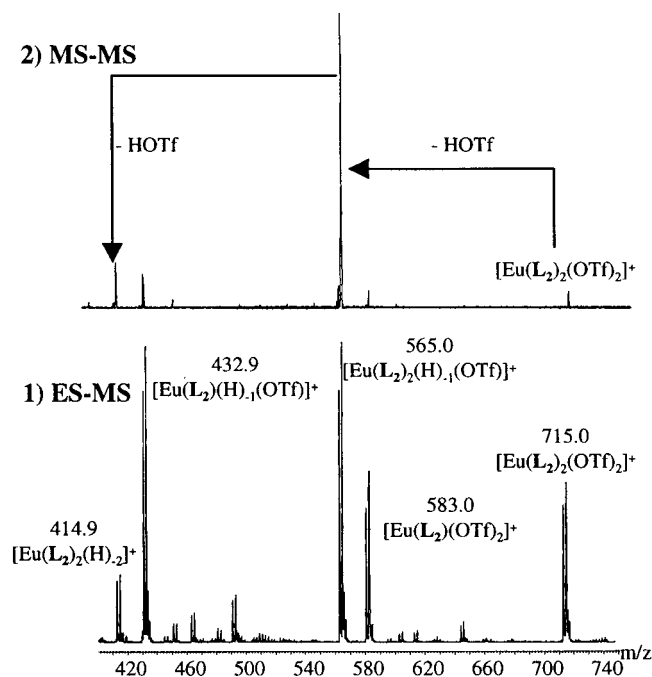


Figure 7. (1) ES-MS and (2) tandem MS spectra of an equimolar sample of L_2 and $\text{Eu}(\text{OTf})_3$ in methanol.

coming from the $\text{Eu}(L)_2$ complexes are seen on the spectra when $\rho = \text{Eu}/L \leq 0.5$; cations coming from the $\text{Eu}(L)$ complexes appear when $\rho = 1$ and become predominant when $\rho = 2$. Third, with nitrates there is always a mixture of ions coming from both complexes, even for $\rho = 0.5$, which confirms the dissociation of $\text{Eu}(L)_2$ complex in methanol. When the cone voltage is increased from 40 to 90 V, intensities of ions of lower mass increase because of anion dissociation ($-\text{HX}$) due to up-front collision.³¹ So as to be sure that the signals in the ES-MS spectra are not due to fragmentation of the molecular ions, we have analyzed the tandem mass spectra (MS/MS) of the $[\text{Eu}(L)_2(X)_2]^+$ cations. As an example, Figure 7 shows the ES-MS and MS/MS spectra of an equimolar sample of L_2 and $\text{Eu}(\text{OTf})_3$. Fragmentation of these cations is only due to successive anion losses ($-\text{HX}$), and very little ligand loss ($-\text{L}$) is detected on the tandem mass spectra. It can then be concluded that ions coming from the $\text{Eu}(L)$ complexes are present in the gas phase and not formed by fragmentation of $\text{Eu}(L)_2$ complexes. Species detected by electrospray mass spectrometry are thus totally in accordance with equilibria deduced from low-temperature ^1H NMR investigations.

(b) $\text{La}(\text{OTf})_3$ Complexation. The ^1H NMR spectra at room temperature of samples containing an equal amount of the ligand (L_1 in acetonitrile- d_3 or L_2 in methanol- d_4) and $\text{La}(\text{OTf})_3$ show clearly the chair interconversion from the free ligand to the complex (Figures 8 and 9). Numbering of protons in ligands L_1 and L_2 throughout the text and figures are respectively depicted in Schemes 2 and 3. The conformational rearrangement of ligand L_1 upon the complexation process is indicated by the evolution of the $^1\text{H}-^1\text{H}$ coupling constants (Figure 8). For example, the axial proton H_1 in the free ligand gives a well-resolved multiplet ($J_{\text{H}_1/\text{H}_3} = 11$ Hz and $J_{\text{H}_1/\text{H}_2} = J_{\text{H}_1/\text{OH}} = 4$ Hz) whereas it is characteristic of an equatorial proton weakly coupled in the complex (large singlet). At low temperature, 233 K, the hydroxyl and H_1 signals both split into two different resonances, indicating the presence of the two complexes $\text{La}(L_1)$ and $\text{La}(L_1)_2$ exchanging in organic solution. This splitting

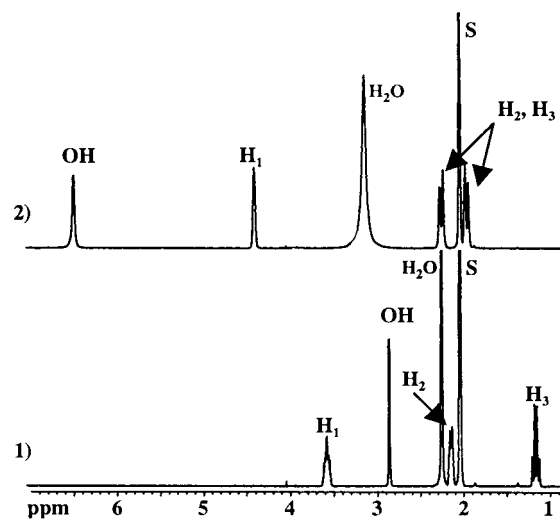


Figure 8. 400 MHz ^1H NMR spectra at 298 K in acetonitrile- d_3 of (1) L_1 and (2) an equimolar mixture of L_1 and $\text{La}(\text{OTf})_3$.

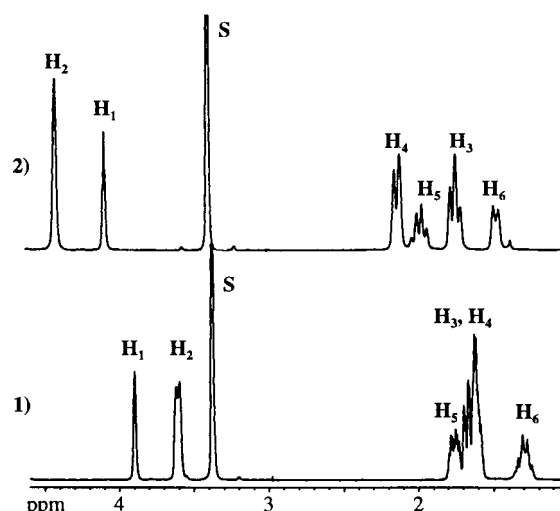
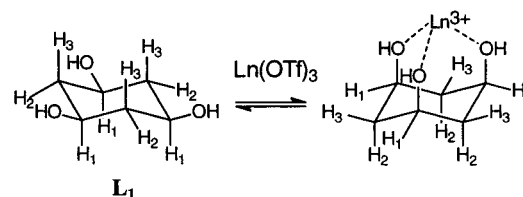
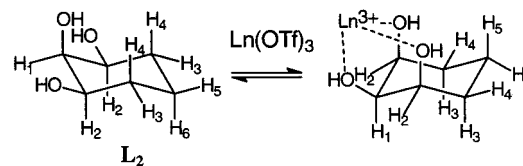


Figure 9. 400 MHz ^1H NMR spectra at 298 K in methanol- d_4 of (1) L_2 and (2) an equimolar mixture of L_2 and $\text{La}(\text{OTf})_3$.

Scheme 2



Scheme 3



does not occur when $\rho = \text{La}/L_1 = 0.5$, and $\text{La}(L_1)_2$ is then the only species observed.

The evolution of the ^1H NMR spectra of L_2 at room temperature upon $\text{La}(\text{OTf})_3$ complexation is shown in Figure 9. In the free ligand L_2 , the axial proton H_2 resonance is a well-resolved multiplet ($J_{\text{H}_2/\text{H}_4} = 10$ Hz and $J_{\text{H}_2/\text{H}_1} = J_{\text{H}_2/\text{H}_3} = 3$ Hz) and it becomes a large downfield-shifted singlet in the complex.

Table 7. ES-MS Intensities of $\text{La}(\text{OTf})_3$ and L_2 Solutions in Methanol^a

species	m/z	$\rho = 0.5$	$\rho = 1$
$[\text{La}(\text{L}_2)_2(\text{OTf})_2]^+$	701	100	39
$[\text{La}(\text{L}_2)_2(\text{H})_{-1}(\text{OTf})]^+$	551	33	15
$[\text{La}(\text{L}_2)_2(\text{H})_{-2}]^+$	401	2	5
$[\text{La}(\text{L}_2)(\text{OTf})_2]^+$	569	17	100
$[\text{La}(\text{L}_1)(\text{H})_{-1}(\text{OTf})]^+$	419	11	52
$[\text{La}(\text{L}_2)(\text{H})_{-2}]^+$	269	8	8

^a Total La concentration = 2×10^{-3} mol L⁻¹. $\rho = [\text{La}]_0/[\text{L}_2]_0$.

At low temperature the ¹H NMR spectrum shows only one set of signals. To determine the number of complexes present in solution, we analyzed the samples by electrospray mass spectrometry under the following stoichiometric conditions: LaL_2 and LaL . Both spectra show the presence of six ions in different proportions (see Table 7). For $\rho = \text{La}/\text{L}_2 = 0.5$, cations coming from the $\text{La}(\text{L}_2)_2$ complex are predominant, and the small amount of ions coming from the $\text{La}(\text{L}_2)$ complex can be attributed to the fragmentation of $[\text{La}(\text{L}_2)_2(\text{OTf})_2]^+$ ($m/z = 701$). The daughters of this species were indeed determined by tandem mass spectrometry experiments that reveal the loss of anions ($m/z = 551$ and 401) and less intensely the loss of a ligand molecule L_2 ($m/z = 569$ and 419). For $\rho = 1$, the proportion of ions coming from the $\text{La}(\text{L}_2)$ complex is much higher and cannot anymore be attributed to fragmentation reactions; both complexes are thus present in the gas phase. This mass spectrometry analysis confirms that lanthanum complexes of L_2 are the same as those observed for europium complexation. The two diamagnetic lanthanum complexes have very close chemical shifts, and are not differentiated by low-temperature NMR.

(c) $\text{Ln}(\text{OTf})_3$ Complexation ($\text{Ln} = \text{Pr, Nd, Yb}$). The same studies by low-temperature ¹H NMR with other lanthanide triflates show that in every cases two complexes are formed in organic solution, with proportions depending on the metal to ligand initial ratio. ¹H NMR spectra at 233 K of samples containing an equal amount of the ligands L_1 or L_2 and the metal triflate are shown respectively in Figures 10 and 11 with the assignments of the two different complexes (**a** is for $\text{Ln}(\text{L}_2)_2$, **b** is for $\text{Ln}(\text{L})$). Assignment of the proton's resonances was realized by 2D NMR correlation spectroscopy: COSY and NOESY spectra. NOESY spectra exhibit only off-diagonal resonances arising from proton exchange between magnetically nonequivalent positions (same sign as the diagonal signals); because of the small proton's relaxation times no through-space interactions (nuclear Overhauser effect) are detected with these three cations. The constant K of equilibrium I at 233 K along the lanthanide series can be evaluated by integrated intensity measurements on the ¹H NMR spectra at low temperature: L_1 (CH_3CN ; $K = 17 \pm 2$ La; 13 ± 1 Pr; 14 ± 1 Nd; 7 ± 1 Eu; 6 ± 1 Yb) and L_2 (CH_3OH ; $K = 140 \pm 30$ Pr; 230 ± 50 Nd; 3.0 ± 0.4 Eu; 270 ± 50 Yb). High uncertainties associated with K determination are due to the low concentration in $\text{Ln}(\text{L}_2)_2$.

Paramagnetic proton relaxation rates allow an evaluation of complex structures in solution. The contact contribution to the lanthanide-induced relaxation rates being negligible compared to the dipolar terms, paramagnetic longitudinal relaxation time is proportional to the sixth power of the lanthanide-proton distances in solution.³⁵ Proton longitudinal relaxation rates could be measured at 400 MHz and 298 K for the $\text{Ln}(\text{L})_2$ complexes, which are the only species in solution for a metal to ligand ratio

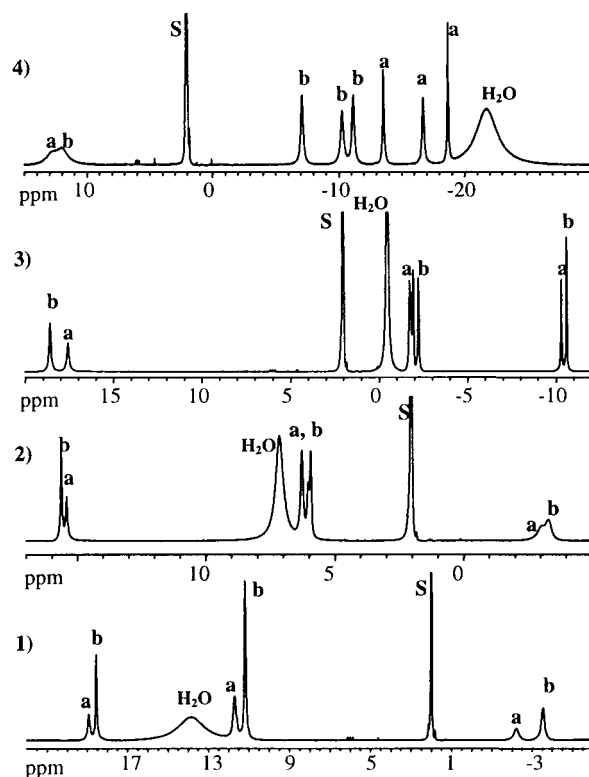


Figure 10. 400 MHz ¹H NMR spectra of equimolecular samples of L_1 and $\text{Ln}(\text{OTf})_3$ at 233 K in acetonitrile- d_3 : (1) Pr, (2) Nd, (3) Eu, (4) Yb (**a**, resonances of $\text{Ln}(\text{L}_2)_2$ complexes; **b**, resonances of $\text{Ln}(\text{L})$ complexes).

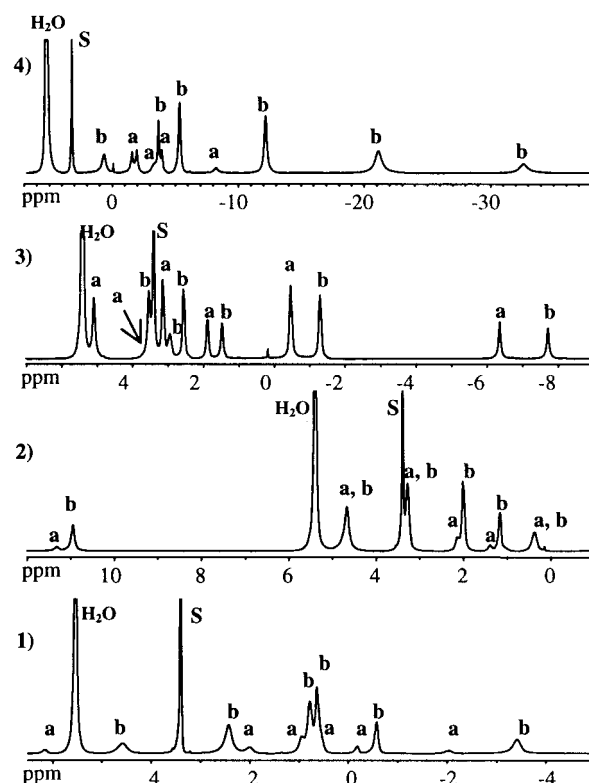


Figure 11. 400 MHz ¹H NMR spectra of equimolecular samples of L_2 and $\text{Ln}(\text{OTf})_3$ at 233 K in methanol- d_4 : (1) Pr, (2) Nd, (3) Eu, (4) Yb (**a**, resonances of $\text{Ln}(\text{L}_2)_2$ complexes; **b**, resonances of $\text{Ln}(\text{L}_2)$ complexes).

(35) Kemple, M. D.; Ray, B. D.; Lipkowitz, K. B.; Prendergast, F. G.; Rao, B. D. N. *J. Am. Chem. Soc.* **1988**, *110*, 8275–8287.

of 0.5. The paramagnetic contributions to these rates are then obtained by subtraction of the diamagnetic term, which is

Table 8. Proton Paramagnetic Relaxation Rates (ms) of Complexes Ln(L₁)₂ at 400 MHz and 298 K in Acetonitrile-*d*₃

Ln	OH	H ₁	H ₂	H ₃
Pr	10	100	<i>a</i>	<i>a</i>
Nd	5	49	<i>a</i>	<i>a</i>
Eu	23	232	398	141
Yb	2	23	53	14

^a *T*₁ not measured because of overlapping signals.

Table 9. Proton Paramagnetic Relaxation Rates (ms) of Complexes Ln(L₂)₂ at 400 MHz and 298 K in Methanol-*d*₄

Ln	H ₁	H ₂	H ₃	H ₄	H ₅	H ₆
Pr	73	48	345	209	92	259
Nd	34	26	175	107	38	252
Eu	102	69	496	284	99	917
Yb	15	<i>a</i>	<i>a</i>	<i>a</i>	<i>a</i>	98

^a *T*₁ not measured because of overlapping signals.

evaluated by the proton longitudinal relaxation rate in the diamagnetic complex La(L₂)₂ (eq 1). Tables 8 and 9 show

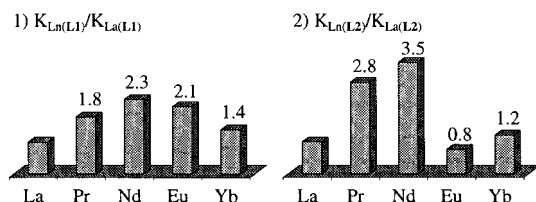
$$\left(\frac{1}{T_1}\right)_{\text{paramagnetic}} = \left(\frac{1}{T_1}\right)_{\text{measured}} - \left(\frac{1}{T_1}\right)_{\text{diamagnetic}} = \frac{A}{r_{\text{Ln-H}}^6} \quad (1)$$

respectively the paramagnetic relaxation times measured for Ln(L₁)₂ in acetonitrile and Ln(L₂)₂ in methanol at 298 K and 400 MHz. The cis/trans position of protons to the paramagnetic center in relation to the cyclohexane ring can be exploited to assign signals in the NMR spectra: protons cis to the metal have shorter relaxation times than those which are trans. Ratios of metal to proton distances in solution obtained from *T*₁ measurements (eq 1) are very close to these ratios calculated in the solid state structures of the crystallized complexes. The distances in the coordination sphere occupied by the two organic ligands in solution are thus very similar to that observed in the solid state.

(d) Selectivity along the Lanthanide Series. The selectivity of these two cyclohexanetriols toward lanthanide(III) can be assessed by performing competition experiments between a ligand and two cations. The ¹H NMR spectra of samples containing the ligand and a 2-fold excess of both lanthanide salts show only the resonances of the two Ln(L) and Ln'(L) complexes. By measuring the integrated intensities on the ¹H NMR spectra we have determined the Ln(L) formation constant ratios *K*_{LnL}/*K*_{Ln'L} (eq 2). Exchange between the two species Ln-

$$\frac{K_{\text{LnL}}}{K_{\text{Ln'L}}} = \frac{[\text{LnL}][\text{Ln}'\text{L}]}{[\text{Ln}][\text{Ln}'\text{L}]} = \frac{[\text{LnL}][\text{Ln}']}{[\text{Ln}'\text{L}][\text{Ln}]} \quad (2)$$

(L₁) and Ln'(L₁) in acetonitrile is slow enough to obtain well-resolved resonances at ambient temperature 298 K, whereas for L₂ complexes in methanol we had to record the ¹H NMR spectra at low temperature, 243 K, to obtain precise integrated intensities. Figure 12 shows the evolution of the formation constants of Ln(L) complexes along the lanthanide series. These constants are calculated relative to that of the lanthanum(III) corresponding complex La(L₁) or La(L₂). Ligand L₁ does not show a pronounced selectivity along the 4f trivalent cation series. The greater constant ratio is 2.3 ± 0.2 for Nd(III) versus La(III). Angyal¹³ had observed that the trihydroxy triaxial site was not very selective toward cations, and molecular mechanics calculations³⁶ have demonstrated that the optimum cation's size for

**Figure 12.** Ln(L) formation constants relative to that of the corresponding La(L) complex (1) for L₁ at 298 K in acetonitrile-*d*₃ and (2) for L₂ at 243 K in methanol-*d*₄.

this triaxial site was 0.63 Å. Lanthanide(III) ions may thus be too large to correctly fit into this 1,3,5-trihydroxy site and to induce a selective recognition. On the other hand, he showed that the 1,2,3-trihydroxy site in the axial-equatorial-axial configuration is more selective toward cations.¹³ Experimental observations and molecular mechanics calculations have shown that the optimum cation's size is about 1 Å, which is close to the trivalent lanthanide ionic radii. The ¹H NMR competition experiments show that L₂ displays a selectivity for the Nd(III) cation, with constants ratios of 3.5 ± 0.3 (Nd versus La) and 4.4 ± 0.4 (Nd versus Eu). It is also interesting to compare these results to the complexation thermodynamic constants of ribose toward lanthanide cations in water measured by microcalorimetry and thin-layer ligand-exchange chromatography (TLC).^{37,38} This sugar exists mainly in aqueous solution as a pyranose form containing the 1,2,3-trihydroxy site³⁹ and is thus comparable to ligand L₂. From La(III) to Tb(III), only 1:1 complexes are formed with ribose and complexation constants vary from 3 to 11 with a maximum for Sm(III). At the end of the series, the constants could not be measured by microcalorimetry but TLC results display a comparable affinity to La(III). These tendencies are very close to that we observed in the case of lanthanide(III) complexation by ligand L₂ in methanol.

Conclusion

This work demonstrates that the two cyclohexanetriols L₁ and L₂, each possessing three hard donor hydroxyl groups, are able to form complexes with trivalent lanthanide cations. Complexation occurs only in organic solvents and not in aqueous solution where water acts as a very strong competitor. The two model molecules L₁ and L₂ are not preorganized, and a conformational chair inversion is thus necessary to organize the three binding oxygen atoms prior to complexation. In water solution, the complex formation does not supply sufficient free energy for the conformational change to take place. At this time, only Ln(L)₂ complexes have been crystallized and 12 structures have been characterized by X-ray diffraction. The only exception is the lanthanum complex 11 which includes both La(L₁) and La(L₂) complexes in the same crystal. The use of low-temperature NMR together with electrospray ionization mass spectrometry has allowed the unambiguous determination of the species present in solution. In contrast to species encountered in the solid state, both complexes Ln(L) and Ln(L)₂ are identified in organic solution for La, Pr, Nd, Eu, and Yb. Competition experiments between two salts show a low selectivity of L₁ along the 4f series. Ligand L₂, which is a model

(36) Hancock, R. D.; Hegetschweiler, K. *J. Chem. Soc., Dalton Trans.* **1993**, 2137–2140.

(37) Morel-Desrosiers, N.; Lhermet, C.; Morel, J.-P. *J. Chem. Soc., Faraday Trans.* **1993**, 89, 1223–1228.

(38) Israëli, Y.; Morel, J.-P.; Morel-Desrosiers, N. *Carbohydr. Res.* **1994**, 263, 25–33.

(39) Morel-Desrosiers, N.; Morel, J.-P. *J. Chem. Soc., Faraday Trans.* **1989**, 85, 3461–3469.

of the *cis,cis*-1,2,3-trihydroxy site found in sugars, shows a better affinity for Nd(III). **L**₂ complexation behavior is very similar to that obtained with ribose which possesses mainly the *cis,cis*-1,2,3-trihydroxy site in water solution. Because the formation constant ratios were not determined in the same conditions (temperature and solvent) for the two ligands, we cannot compare their selectivities along the lanthanide series. We are now planning to obtain more efficient ligands derived from **L**₁ and **L**₂ by introducing well-positioned alkyl chains on the cyclohexane ring so as to preorganize the donor atoms prior to complexation. Lanthanide complexation studies by *cis*-inositol, which contains both 1,3,5-triaxial and 1,2,3-axial, equatorial, axial coordination sites simultaneously preorganized, will also allow us to compare the affinity of the two trihydroxy sites.

Acknowledgment. The authors thank the Direction du Cycle du Combustible at the Commissariat à l'Énergie Atomique for financial support.

Supporting Information Available: Table S1 (elemental analyses); Figure S1 (400 MHz ¹H/¹H NOESY NMR spectrum of an equimolecular sample of **L**₂ and Yb(OTf)₃ at 243 K in methanol-*d*₄ (mixing time 10 ms)); Figure S2 (400 MHz ¹H/¹H NOESY NMR spectrum at 243 K in methanol-*d*₄ of a 2:2:1 mixture of respectively Nd(OTf)₃, Eu(OTf)₃, and **L**₂ (mixing time 50 ms)); and X-ray crystallographic files, in CIF format, for the structures of complexes **1**, **2**, **4**, **5**, **6**, **8**, **9**, **11**, and **12**. This material is available free of charge via the Internet at <http://pubs.acs.org>.

IC001160E